Excited state charge separation in symmetrical alkenes

Zijlstra, Robert Wiebo Johan

Solvent-Induced Charge Separation in the Excited States of Symmetrical Ethylene:

A Direct Reaction Field Study

4.1 Introduction

One of the most fundamental processes in chemistry is the photo-induced cis-trans isomerization involving an olefinic double bond[1]. The importance of this process is illustrated by its presence in a large number of biological systems, for instance the ultra-fast cis-trans isomerization in the retinal chromophore of rhodopsin which triggers a series of events ultimately leading to vision in mammals[2, 3]. An overwhelming number of both theoretical[4-26] and experimental[3, 27-56] studies focussing on the dynamics, lifetimes and electronic features of these isomerizations in a wide variety of olefins has been performed in order to gain deeper insight in this process.

The first study of the electronic features of cis-trans isomerizations dates back to 1932 when Mulliken[1] predicted that the (π,π->π,π^*) excited state should undergo a large intramolecular rearrangement due to rotation around the ground state double bond from a planar ground state geometry to a (near) perpendicular excited state geometry, the so called phantom state[57]. By now it is well accepted that the driving force behind this conformational relaxation is the reduction of the bond order in this bond accompanied by the repulsion of the two 'non-bonding' π-electrons and the opposite substituents on either side of the double bond.

An interesting feature of this rearrangement is the possible occurrence of an avoided crossing between the S_1 (π,π^*) and S_2 (π^*,π^*) surfaces in the vicinity of the phantom state geometry. On the basis of a simple two electrons in two orbitals description it was suggested that the determinants that give rise to these singlet excited states should be of ionic character (a^2, b^2)[1, 57]. As a consequence, the avoided crossing can lead to the occurrence of large dipole moments in situations where, due to symmetry breaking by for instance asymmetric substitution, the equivalence in the weight of both determinants is no longer present. Therefore even D_2 symmetrical alkenes, which lack a permanent dipole moment in their ground state configuration, can exhibit large dipole moments in their relaxed excited states geometries.

A large number of both experimental[28, 29, 35, 39, 43, 44, 47, 50, 53, 56] and theoretical[4, 10, 13, 16, 24, 58-60] studies have been performed in attempts to gain both experimental evidence as well as additional information about the driving forces governing this symmetry breaking, which is often referred to as sudden polarization[5], especially in the condensed phase.

The most direct evidence for the charge transfer (CT) character of the tetraphenylethylene (TPE) relaxed excited state has been reported by Schuddeboom et. al., who performed Flash-Photolysis Time-Resolved-Micro-Conductivity (FP-TRMC) experiments[44]. A considerable increase in microwave absorption was observed upon excitation of the TPE with a laser pulse, which is indicative of a highly dipolar excited state.

Other studies on TPE have revealed a strong correlation between the lifetime of this polarized excited state and solvent polarity. A spectacular drop in lifetime is observed when the solvent becomes more polar. Schilling and Hilinsky observed a dramatic drop in TPE excited state lifetime from several nanoseconds in non-polar solvents to only a few hundreds of picoseconds in (di)polar solvents[35]. Picosecond optical calorimetry studies by Ma et al. showed a decrease of the energy gap between ground and excited state of several (*para*-substituted)-TPEs with increasing solvent polarity, which has led to the

suggestion that the energy difference between ground and excited state is a measure for the coupling between the two states, thus explaining the decrease in lifetime of CT states in polar solvents[43, 47].

The avoided crossing has also been suggested to play an important role in the isomerization of retinal which indicates the generality of its occurrence in cis-trans isomerizations[3].

From a theoretical point of view, various attempts have been made to describe the process of sudden polarization in symmetrical alkenes. Several configuration interaction (CI) studies on ethylene[10, 13] have shown that at (near) perpendicular geometries three important singlet states arise; the N state, which is the biradicaloid ground state at this geometry, and the ionic Z and V states, these states become degenerate at a central bond twist angle of about 80°. In the vicinity of this degeneracy, lowering of the nuclear symmetry by pyramidalizing one of the carbon centers leads to the formation of considerable dipole moments in the Z and V state of ethylene.

These calculations in vacuum clearly point out the necessity of symmetry breaking to allow polarization to occur, in this case achieved by lowering the nuclear symmetry of ethylene. It was concluded from these studies that at (near) perpendicular geometries, the lowest energy conformation of the ethylene excited state must be of a zwitterionic nature and only exhibit C_s symmetry . The outcome of these studies has led to the general belief that intramolecular symmetry breaking (e.g. the pyramidalization of one of the two carbon centers forming the central olefinic bond) is an exothermic process and, for that reason, the twisted excited state of these olefins is of an *intrinsically* zwitterionic nature[44], where the solvent dependent lifetimes are caused by the more effective stabilization of the zwitterion by more polar solvents[39]. This would lead to shorter lifetimes due to the narrowing of the gap between the photo-excited and ground state potential energy surfaces and hence to an enhanced radiationless transition rate. However, these assumptions are not supported by the work presented in chapter 2, where it was suggested that an increasing size of the functional groups attached to the carbons forming the olefinic bond reduces or even prohibits the stabilization of the zwitterionic excited state by intramolecular symmetry breaking (i.e. pyramidalization).

In addition, numerous spectroscopic studies on for instance *cis*-stilbene[40] and TPE[28, 29, 43, 56] indicate that the observed solvatochromic dependence of the excited state behavior cannot be explained by pure charge transfer (CT) character in all cases. In fact, the CT state in such systems is only effectively populated in polar solvents, as was recently demonstrated by means of femto-second pump-probe experiments on TPE[56](see also chapter 5). These studies revealed that for nonpolar solvents an equilibrium exists between a nonpolarized, charge-resonant (CR) state and the CT state of TPE, which is in good agreement with earlier suggestions of a similar nature[29, 50]. It should be noted that in the work presented here this nonpolarized excited state is addressed to as a charge resonant (CR) rather than a biradical state. It is emphasized that, due to the ionic nature of the determinants involved in the description of these excited states, the names 'biradical' or 'biradicaloid structure' are at best misleading. The term 'biradical' is only an appropriate nomenclature for the near-degenerate states described by the ^{1}ab and ^{3}ab determinants at the phantom state geometry, for which the singlet-triplet splitting is small. A more extensive discussion on the nomenclature of the involved states can be found in chapter 5.

Based on the observed solvatochromic excited state CT behavior of (for instance) TPE in the experiments mentioned above, it should be interesting to investigate the solvent induced charge separation in the (in vacuo) charge symmetrical excited states of the parent alkene ethylene. In the condensed phase, the necessary lowering of symmetry is automatically provided by the finite number of solvent molecules surrounding the solute, leading to a low symmetry environment of the ethylene. It is therefore worthwhile to investigate the ability of various solvents to provide enough symmetry breaking to generate the charge separated states.

It has been shown in the previous chapter, by enveloping ethylene with a Connolly surface[61] carrying a nonsymmetrical distribution of dipole densities (i.e. a model for a solvent in equilibrium with a polarized solute), that an increase of the dielectric constant of the continuum leads to more pronounced polarization as well as stabilization for the ethylene excited states[24].

In this chapter the results of a study of the ability of several organic solvents with varying polarity as well as polarizability to "suddenly" polarize the ethylene excited states at near perpendicular geometries will be presented.

In order to achieve this the Direct Reaction Field (DRF) method has been employed. The DRF method is a hybrid quantum mechanical/classical (QM/MM) method for including the effect of surroundings, e.g. a solvent shell in quantum chemical calculations[62-64]. In this method the system of interest (in this case the ethylene) is described quantum mechanically using an ab initio or semi-empirical wave function whereas the surroundings are described classically by means of point charges and explicit polarizabilities. The DRF method is briefly discussed below.

It will be shown that increasing solvent polarity not only increases the expectation value of the ethylene dipole moment but that even for non-equilibrium solvent surroundings (i.e. a solvent in equilibrium with a non-polarized charge distribution of the ethylenic excited state) a distinct stabilization of the charge separated excited state can occur.

4.2 Description Of The Calculations

4.2.1 Direct Reaction Field Calculations

The DRF method combines a quantum mechanical description of a solute with a classical description of its surroundings and is schematically shown in Figure 3.1. This method has been extensively described in several publications[62-66] as well as in chapter 3. Therefore, only some specific issues that are relevant to the work presented here, will be discussed.

The computational level that is used to describe the quantum system in the DRF method can be of arbitrary complexity. The DRF method has been implemented for a number single determinant ab initio methods, e.g. Restricted Hartee-Fock (RHF) and Restricted Open Shell Hartree-Fock (ROHF) as well as for multi-determinant methods like Configuration Interaction (CI). The latter type of wavefunction is of obvious importance for the description of excited states and will be used in the present study.

The solvent molecules surrounding the 'quantum system' are described classically by a set of point charges and explicit polarizabilities centered on all atomic centra. The whole system (quantum mechanical and classical) can optionally be surrounded by a dielectric continuum for modeling bulk effects. The point charges used in this study were obtained by fitting to electrostatic potentials obtained from Hartee-Fock calculations in points selected according to the CHelpG scheme using Dunnings cc-pVDZ basis set[67]. The atomic polarizabilities used here were taken from an extensive study by Van Duijnen and Swart[68] who optimized the values used in the DRF method by fitting to a set of experimental polarizabilities according to a method developed by Thole[69]. The actual values of all parameters used are listed in the Appendix.

For the present study the ethylene (quantum system) was surrounded by 50 classical solvent molecules modeling approximately the first three solvent shells. A set of more or less random solvent shells was generated by performing fully classical Monte Carlo (MC) calculations[70] using the DRF force field. After equilibration, a simulation of 200,000 MC steps was performed from which 20 randomly chosen solvent conformations were saved for the actual QM/MM analysis. The whole system was constrained to a spherical cavity with a radius chosen to obtain the experimental density.

In these simulations the ethylene solute was also treated classically by fitting it with charges and polarizabilities in its vacuum (i.e. nonpolarized) N-state. This way it was assured that any polarization arising in the ethylene excited states can be regarded as "sudden" since the solvent shells represent the equilibrium surrounding of the nonpolarized ethylene.

The above described procedure was performed using ethane, tetrachloromethane, chloroform, acetone and carbon dioxide (CO_2) as solvents. All of these solvents have little internal degrees of freedom which make them attractive solvents for the MC sampling since the internal degrees of freedom can be omitted in these simulations. The choice of ethane and carbon dioxide as solvents deserves some further explanation since both of them are gases at ambient conditions. Ethane can be considered as a model system for nonpolar hydrocarbons like *n*-hexane but has the advantage of little internal degrees of freedom. Additionally, supercritical ethane has been used in experimental studies by Sun et al.[50] on the charge separation behavior of TPE and it was found that its effect on the CT character and excited state lifetime was comparable to that of *n*-hexane. Supercritical carbon dioxide was also used in the same study and despite its lack of a permanent dipole moment it was shown to exhibit behavior that is typical for polar solvents.

The influence of the different solvent configurations on the polarization and stabilization of the excited states of ethylene was investigated by performing mixed QM/MM calculations on the 20 solvent conformation obtained from the classical MC simulations The ethylene was described using a CI wavefunction including all single and double excitations from the valence orbitals using the vacuum orbitals of the N-state as the reference determinant (CISD). These reference orbitals were obtained from a singlet ROHF calculation using Dunning's DZV basis set[67]. Such a procedure is known to produce perfectly zero dipole moments[24] in vacuum which is an obvious requirement for the present study.

The use of a multi-determinant wavefunction in the DRF method introduces a complication for the evaluation of the dispersion contribution to the interaction energy between the quantum system and the classical solvent. This becomes evident when

considering the DRF-definition of the interaction energy between the classical system and single determinant wave function:

$$\Delta U_{int}^{QM/MM} = \sum_{A,i,j} q_i^A \vartheta_{ij} Z_j + e \sum_{A,i} q_i^A \langle \vartheta \rangle_i +$$
$$\sum_{A,i,j,r,s} q_i^A f_{ir} A_{rs} f_{sj} Z_j + e \sum_{A,k,j,r,s} q_j^A f_{jr} A_{rs} \langle f(s;k) \rangle +$$
$$\frac{1}{2} \sum_{i,j,r,s} Z_i f_{ir} A_{rs} f_{sj} Z_j + e \sum_{i,k,r,s} Z_i f_{ir} A_{rs} \langle f(s;k) \rangle + \quad \textbf{(4.1)}$$
$$\frac{\gamma}{2} e^2 \sum_{k,r,s} \langle f(k;r) A_{rs} f(s;k) \rangle + \frac{1}{2} e^2 \sum_{k,l,r,s} \langle f(k;r) \rangle A_{rs} \left(1 - \frac{\gamma}{2} P_{12} \right) \langle f(s;l) \rangle$$
$$+ \Delta U_{rep}^{QM/MM}$$

In this expression the first two terms describe the electrostatic interaction of the nuclei and electrons with the point charges of the solvent. The next two terms describe the interactions between the point charges and the dipoles induced by the nuclei and electrons and vice versa. The fifth and sixth term represent the screening of the nuclear repulsion and attraction, respectively. The seventh and eighth term describe the interaction of an electron with its own and the other electrons' induced dipole moments, the latter term is therefore a two-electron term which contains the induction and part of the dispersion interaction. The scaling factor γ is used for the dispersion and was shown to be roughly equal to the following expression including the second order perturbation theory expression (SOP) for the dispersion[66]:

$$\Delta U_{disp}^{SOP} \approx \left(\frac{E_{solvent}^i}{E_{solute}^i + E_{solvent}^i} \right) \Delta U_{disp}^{DRF} = \gamma \Delta U_{disp}^{DRF} \quad \textbf{(4.2)}$$

The scaling factor γ can be used to redefine the reaction field operator by scaling the integrals for the screening of the one-electron self-energy as well as the two-electron exchange contributions. The latter rescaling is only then possible when the exchange interaction is explicitly defined, i.e. when dealing with a single determinant wavefunction. The present calculations were therefore performed using $\gamma = 0$.

An estimate of the dispersion interaction was added afterwards by performing a series of separate DRF calculations on the R(O)HF wavefunctions corresponding to the three dominating determinants (a^2, b^2 and ab; the two zwitterionic and the biradical determinants) of the CI wavefunction.
These wave functions were constructed from the vectors used in the CI calculations in the corresponding solvent configurations without allowing orbital relaxations, ensuring the use of the same MO space in the estimation of the dispersion contributions. The thus obtained dispersion contributions were weighted by the normalized CI coefficients of the corresponding determinant.

Solvent	Ionization Potential (eV)	γ (with ethylenic N / Z,V state)
ethane	11.5	0.540 / 0.647
tetrachloromethane	11.47	0.539 / 0.646
chloroform	11.42	0.538 / 0.645
carbondioxide	13.77	0.584 / 0.687
acetone	9.69	0.497 / 0.609
ethylene (N state / Z,V state)	9.80 / 6.28	--

Table 4.1 Ionization potentials and resulting γ of applied solvents and perpendicular ethylene.

For the ionization potentials of the solvent molecules used in equation 4.2 experimental values were taken[71]. The ionization potentials of the various states of ethylene in its twisted geometry had to be determined theoretically, since for obvious reasons experimental data is lacking. The ionization potential of the biradical was extracted from two successive ROHF calculations, the first one describing the full electron configuration at this geometry and the second one in which one electron was removed from the system without allowing orbital relaxations. The difference between these two energies can be used as an estimate of the vertical ionization potential of the N-state of ethylene. The ionization potential of both the Z and V state, which were taken to be degenerate, was obtained by taking the excitation energy (energy difference between the N-state and the Z and V states) from the vacuum CISD calculations described above and subtracting it from the ionization potential of the N-state. The ionization potentials obtained in this way can be considered reasonable estimates of the ionization potentials of twisted ethylene in the N, V and Z states and are listed in Table 4.1 together with the values for the scaling factor γcalculated according to Eq. 2.

4.2.2 The Ethylene Geometry

The geometry of ethylene used in this study is shown in figure 4.1. Bond lengths and angles were taken from a RHF geometry optimization using a basis set of double zeta quality including polarization functions. In the present work all calculations were performed using a single twist angle (i.e. the H-C-C-H dihedral angle) of 81˚ which was found to be the angle where the maximum excited state polarizability occurs (*vide infra*) and therefore the maximum polarization effect can be expected at this angle.

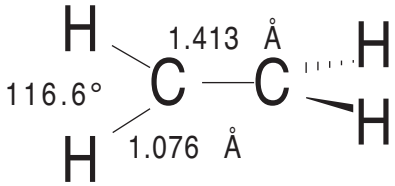

Figure 4.1 Adopted ethylene geometry.

It is questionable whether the explicit investigation of several ethylene geometries (i.e. at various twist angles) would provide valuable additional information, as the results from the study presented in chapter 3, where a polarized dielectricum only as a surrounding was used, already pointed out that this angle had a distinct optimum value for the polarizability of the excited state(s) regardless of the ε applied. Deviations from this value are likely to provide less explicit polarizations of the ethylene excited state charge density which for instance is shown by FFPT calculations in which the polarizability as a function of the twist angle near the perpendicular geometry is investigated for the electronic states of interest (*vide infra*).

The most suitable value for this twist angle has to be determined carefully to ensure the optimal response of the ethylene polarizability towards symmetry breaking by the solvent shells. In other words, the region for the highest probability of the avoided crossing has to be determined.

Although the most appropriate value for this property already has been the subject of previous studies[10, 13], the drawback there was that these calculations were performed without an external perturbation (for instance an electric field) applied to the wave function of the ethylene. Since this study is focussed on the likelyhood of sudden polarization occurring on the excited state potential energy surface of the twisting ethylene it was decided to include such effects in the determination of the ideal candidate geometry for this study.

To this purpose, a finite field (FFPT) calculation[72, 73] at the CISD level in the DZV basis[67] using HONDO 8.1[74] was employed by which the polarizability of the ethylene ground and excited state potential were calculated as a function of the abovementioned twist angle from the Taylor expansion of the total dipole moment:

$$\mu_j = \mu_{j,0} + \alpha_{ji} \cdot F_i + \frac{1}{2} \cdot \beta_{jii} \cdot F_i^2 + \frac{1}{6} \cdot \gamma_{jiii} \cdot F_i^3 \ldots \qquad \textbf{(4.3)}$$

Twist angles from 70 to 90˚ have been examined and polarizabilities of both ground and first excited state have been determined by taking steps of 1˚ in this region. From this work as well as from the earlier mentioned study using a polarized dielectricum only as environment, the $H_aC_a—C_bH_b$ dihedral angle was set to 81˚ (*vide infra*).

4.3 Results and Discussion

4.3.1 Polarizability of Ethylene Excited States at Different Twist Angles

The finite field method was used to calculate the polarizability of the first excited state of ethylene in the 70-90° twist area. Initial calculations using field strengths of ~ 10^{-4} a.u. revealed a strongly non-linear behavior of the polarizability component along the C-C bond at a twist angle of 81˚ as evident from Figure 4.2. An induced dipole moment of 2.8 Debye is obtained at a field strength of $5*10^{-5}$ a.u., further increase of the electric field increases the dipole moment only slightly. Thus the electric field of $5*10^{-5}$ a.u. is already sufficient to cause an energy difference between the two carbon atoms that is large enough for a full charge separation to occur.

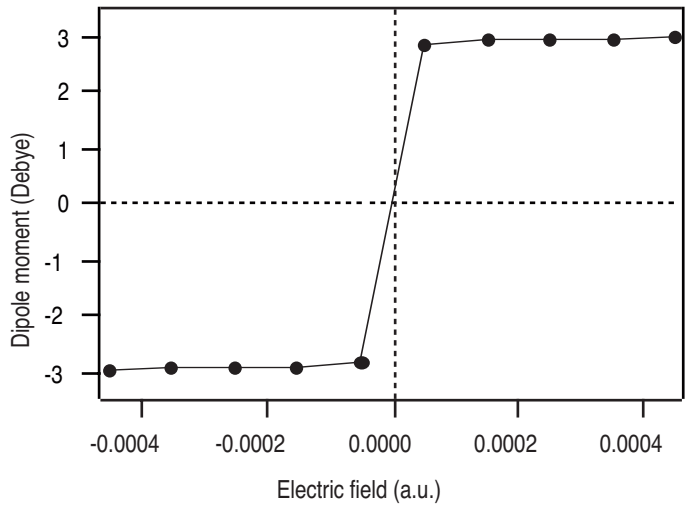

Figure 4.2 Induced dipole moment of the first excited state of 81˚ twisted ethylene.

Further calculations were performed using electric fields strengths of the order of 10^{-6} a.u., at these values the induced dipole moment was found to depend linearly on the electric field. The results obtained from these calculations for the component of the polarizability along the C-C axis at various twist angles are shown in figure 4.3.

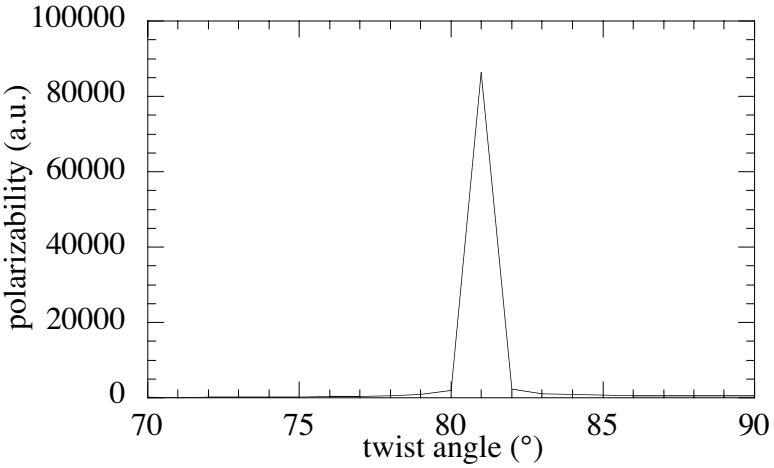

Figure 4.3 Polarizability component (a.u.) along the C-C axis of the first excited state of twisted ethylene as a function of the twist angle in the 70-90˚ range.

The largest polarizability was found for near-perpendicular ethylene with a twist angle of 81°. However, the dramatic increase shown in figure 4.3 should be interpreted with some caution, since the (near-)degeneracy of the Z and V surfaces in the vicinity of this geometry leads to a heavy mixing of both states resulting in an avoided crossing area for which the Born-Oppenheimer approximation no longer holds. Inclusion of the coupling between electronic and nuclear motion in the wavefunction (as for instance in a quantum dynamical treatment) would lead to a better description of the phenomenon but is beyond the scope of this work.

These finite field calculations clearly point out that, within the theoretical framework of choice in this study, the degeneracy of the Z and V surfaces leading to the enhanced excited state polarizability occurs around the 81˚ twist angle. Therefore, the twist angle was set equal to this value in the remainder of the work presented here.

4.3.2 Solvent-Induced Charge Separation in Twisted Ethylene

The solvent induced dipole moments along the central C-C bond obtained from the DRF calculations described above are listed in Table 4.2 for the three states of interest. These values represent the absolute value for the dipole moment averaged over the 20 CI calculations with different solvent conformation. In reality, the calculated values exhibit both positive and negative values, dependent of the direction of the effective (static) field of the surrounding solvent. Averaging over the actual values would result in near-zero dipole moments, which is undesirable here since this provides no insight into the magnitude of the polarization of especially the excited states (states 2 and 3) of the twisted ethylene.
In all the CI calculations, the dipole moments along the z-axis of the two excited states within a single calculation were of opposing signs, a direct result of the orthogonality (a^2 vs. b^2) of the two (heavily mixed) states.

	$\|\mu_z\|$ (Debye) state 1	$\|\mu_z\|$ (Debye) state 2	$\|\mu_z\|$ (Debye) state 3
ethane	0.00 (*±0.00*)	0.09 (*±0.06*)	0.08 (*±0.06*)
tetrachloromethane	0.01 (*±0.01*)	0.72 (*±0.46*)	0.70 (*±0.44*)
chloroform	0.05 (*±0.05*)	2.07 (*±0.92*)	1.93 (*±0.82*)
carbon dioxide	0.09 (*±0.06*)	2.62 (*±0.75*)	2.37 (*±0.59*)
acetone	0.10 (*±0.05*)	2.61 (*±0.66*)	2.38 (*±0.53*)

Table 4.2 Average solvent induced dipole moments (μ_z, absolute values) of the three roots of interest in the 81˚ twisted ethylene. Standard deviations shown in parenthesis.

The most interesting feature that can be observed from the results in Table 4.2 is the distinct difference in expectation values of the dipole moments of the, in vacuum, near-degenerate Z and V states (states 2 and 3) in non-polar and polar solvents. In the non-polar solvents ethane and tetrachloromethane the induced dipole moments of these states are relatively small, especially in ethane (~±0.1 D). In tetrachloromethane, slightly larger dipole moments (~0.7 D) are induced, although the spread (standard deviation) in the values is rather large (~0.45 D). In fact, dipoles ranging from approximately 0.2 to 1.6 Debye were obtained from the various calculations using tetra as a solvent. This indicates that an asymmetric distribution of polarizabilities around the ethylene can sometimes introduce enough symmetry breaking to induce charge separation, even if no permanent electric field is present.

The excited states of the twisted ethylene exhibit larger dipole moments in the more polar solvents. In chloroform, which exhibits medium polarity, the average dipole moments are already 2.0 D, although the spread is still large (~ ±0.9 D). Calculated dipoles ranged from 0.1 to 3.2 D, indicating that large polarization can take place in certain but not all solvent geometries.

When looking at CO_2 and acetone, induced dipole moments in the excited states are very large (~ 2.6 D) with a small spread compared to that of the less polar solvents (~ ±0.6 D; under 25% of the average induced dipole moment), indicating that in (nearly) every solvent configuration large excited state polarization is achieved. For instance, in acetone the excited state dipole moments are mainly ranging between 1.8 and 3.3 D.

Observations for the 'ground' state (state 1) are less dramatic; moderately small polarizations up to 0.1 D in acetone are found and show the expected correlation with increasing solvent polarity (or polarizability) and will not be discussed any further.

The results presented above clearly demonstrate that there is a relation between the nature of the solvent and the magnitude of symmetry breaking in the ethylenic excited states. In order to gain deeper insight in the origin of this relation a more detailed look into the interactions between the various electronic states of the twisted alkene and its solvent-surroundings is necessary.

Tables 5.3 to 5.8 specify the total interaction energy as well as the various components of that energy of the three states of interest of the 81˚ twisted ethylene with ethane, tetrachloromethane, chloroform, carbon dioxide and acetone respectively.

Four components contributing to that energy are specified:

- The electrostatic interaction (ΔE_{elec}), which is the interaction between the permanent charge distribution of the quantum system with the static charge distribution of the solvent.
- The dispersion interaction (ΔE_{disp}) between the quantum system and the solvent.
- The induction interaction (ΔE_{ind}), which is the interaction between the permanent charge distribution of the quantum system with the dipole moments it induces in the classical system.
- The polarization energy (ΔE_{pol}) consist of three contributions; the interaction between the quantum system and the moments induced by the classical charge distribution in the classical system (1), the interaction between the classical charge distribution and the moments that the quantum system induces in the classical system (2), and the cost of inducing all the dipoles in the classical system.

Note that this kind of decomposition is rather arbitrary since the 'permanent' charge distribution of the quantum system depends very much on the solvent surrounding it as shown above, however, this polarized charge distribution is taken as the permanent charge distribution for the evaluation of ΔE_{elec}. The tables also include an estimate of the short range repulsion interaction (ΔE_{rep}), this interaction between the quantum system and the classical surroundings is evaluated fully classically in the present implementation. Therefore this contribution is the same for all states. Furthermore, it should be realized that this contribution is not 'felt' by the electrons in the quantum system and is only included to get an estimate of the total interaction energy. For the evaluation of the interaction difference between different states it is irrelevant.

The main advantage of being able to breakdown the total interaction energy into its separate physically relevant components is that the origin of possible state particulate interactions can be detected.

	State 1	State 2	State 3
ΔE_{tot}	**-3.25**	**-4.77**	**-4.71**
ΔE_{rep}	4.23	4.23	4.23
ΔE_{pol}	0.02	0.03	0.03
ΔE_{ind}	-0.04	-0.06	-0.07
ΔE_{elec}	0.00	0.00	0.00
ΔE_{disp}	-7.46	-8.97	-8.90

Table 4.3 Various averaged contributions to the average total interaction energy of the three roots of interest in the 81° twisted ethylene with ethane (kcal·mol^{-1}).

Table 4.3 shows the interaction energies of the three electronic states of interest of ethylene in ethane solution. It clearly shows that for all states the only significant stabilizing contribution to the interaction energy is the dispersion interaction, which is therefore solely responsible for the larger interaction of the excited states with the solvent. No significant charge separation takes place in this solvent and therefore the electrostatic contribution to the interaction energy is zero. The same applies of course to ΔE_{pol} and ΔE_{ind}.

In the case of tetrachloromethane, similar observations can be made (Table 4.4). Again, the dispersion term is the only significant contribution to the interaction energy of each state. Only a very small increase is observed in the electrostatic interaction between the first excited state (root 2) and tetrachloromethane when compared with ethane, this is the interaction of the charge separated ethylene with the point charges that model the tetrachloromethane. This small charge separation is caused by the asymmetric distribution of polarizabilities around the ethylene as argued above.

In the weakly polar chloroform, some significant differences with the earlier discussed solvents occur (table 4.5). The dispersion interaction still is the main contributor to the total interaction energy. No significant difference in dispersion interaction occurs between the two excited states which was the same for the previous solvents.

However, here for the first time a significant difference in electrostatic interaction with the solvent occurs for these states. The first, lower lying excited state has an attractive interaction with the solvent, whereas the state with the roughly equal but opposing dipole moment has a repulsive electrostatic interaction with the field.

	State 1	State 2	State 3
E_{tot}	**-0.99**	**-1.69**	**-1.69**
ΔE_{rep}	2.44	2.44	2.44
ΔE_{pol}	0.01	0.03	0.03
ΔE_{ind}	-0.01	-0.05	-0.06
ΔE_{elec}	-0.03	-0.06	0.00
ΔE_{disp}	-3.40	-4.05	-4.10

Table 4.4 Various averaged contributions to the average total interaction energy of the three roots of interest in the 81° twisted ethylene with tetrachloromethane (kcal·mol^{-1}).

This can be rationalized by realizing that the solvent shell, especially in the case of a polar solvent, introduces an electric field with a more or less random direction at the position of the twisted ethylene solute. This field will in general have some component along the C-C bond of the ethylene which causes charge separation to occur if the field is large enough.

This leads to two charge separated stated with opposing dipole moments. The lowest of these states will have an attractive electrostatic interaction with the solvent which lowers its energy whereas the higher one has a repulsive interaction with the static field of the solvent and hence its energy increases.

	State 1	State 2	State 3
$\mathbf{E_{tot}}$	**-1.93**	**-3.31**	**-2.33**
ΔE_{rep}	2.62	2.62	2.62
ΔE_{pol}	0.02	0.25	0.11
ΔE_{ind}	-0.02	-0.37	-0.32
ΔE_{elec}	-0.13	-0.75	0.38
ΔE_{disp}	-4.42	-5.06	-5.12

Table 4.5 Various averaged contributions to the average total interaction energy of the three roots of interest in the 81˚ twisted ethylene with chloroform ($kcal \cdot mol^{-1}$).

As a result, the interaction with the solvent removes the degeneracy between the two excited states. The equilibrium electronic state of ethylene will therefore shift towards the polarized shape, unlike the case of ethane and tetra, where both excited states stay more or less degenerate. It can be seen in table 4.5 that there is also a contribution from the induction interaction to the total interaction energy, the magnitude of this component is similar for both the excited states which indicates that the magnitude of the dipole moments is about the same (see also Table 4.2) but they have opposing directions.

	State 1	State 2	State 3
$\mathbf{E_{tot}}$	**-4.09**	**-7.22**	**-4.77**
ΔE_{rep}	3.57	3.57	3.57
ΔE_{pol}	0.07	0.59	0.26
ΔE_{ind}	-0.05	-0.82	-0.67
ΔE_{elec}	-0.64	-2.26	0.33
ΔE_{disp}	-7.04	-8.30	-8.26

Table 4.6 Various averaged contributions to the average total interaction energy of the three roots of interest in the 81˚ twisted ethylene with carbon dioxide ($kcal \cdot mol^{-1}$).

For the polar solvents CO_2 and acetone (tables 4.6 and 4.7) the results are quite similar and resemble those found for chloroform. The dispersion interaction dominates the interaction energy of all states. The main difference with chloroform is the magnitude of the electrostatic interaction. This contribution is much larger in CO_2 and acetone for the second state (the first excited state). For CO_2 this may seem surprising because CO_2, unlike chloroform, does not exhibit a permanent dipole moment. However, CO_2 does have

a large quadrupole moment which apparently is enough to provide substantial electrostatic interactions with the induced ethylenic dipole moments. For acetone the contribution of the induction interaction is somewhat larger (for both excited states), probably because of the larger polarizability of acetone.

The marked difference in the polarization and stabilization of the ethylene excited state in ethane and CO_2 provides an explanation for the experimentally observed shortening of the TPE excited state lifetime in supercritical CO_2 compared to supercritical ethane by Sun et al.[50]

	State 1	State 2	State 3
$\mathbf{E_{tot}}$	**-3.81**	**-9.13**	**-6.38**
ΔE_{rep}	8.06	8.06	8.06
ΔE_{pol}	0.09	0.85	0.46
ΔE_{ind}	-0.07	-1.44	-1.15
ΔE_{elec}	-0.41	-2.49	0.27
ΔE_{disp}	-11.48	-14.11	-14.02

Table 4.7 Various averaged contributions to the average total interaction energy of the three roots of interest in the 81° twisted ethylene with acetone (kcal·mol^{-1}).

In CO_2, an additional stabilization of 1.5 kcal·mol^{-1} is observed for the second state (the first excited state) compared to the ground state which lowers the energy gap and therefore leading to an enhanced radiationless crossing rate between the two states, resulting in a shortening of the excited state lifetime. It should be emphasized that the solvent shells used here are in equilibrium with the non-polarized ethylene charge distribution (i.e. the ground state), which means that a considerable additional stabilization of the polarized excited state can be expected upon relaxation of the solvent on the polarized charge distribution of the ethylene. This will further decrease the excited state life time. This additional stabilization is absent in ethane.

Table 4.8 summarizes the solvent effect on the energy difference between the three states studied in this work. Negative values indicate a decrease in the energy gap between the two states whereas positive values represent an increase. The energy gap between the ground state and the first excited state decreases in all solvents. This is mainly caused by dispersion interactions as argued above. This dispersion contribution is always larger in the excited states, and hence lowers the energy gap.

	$\Delta\Delta E_{int}$ (kcal.mol^{-1}) (root 1-root 2)	$\Delta\Delta E_{int}$ (kcal.mol^{-1}) (root 2-root 3)
ethane	-1.52	0.00
tetrachloromethane	-0.70	0.00
chloroform	-1.78	+0.98
carbon dioxide	-3.13	+2.45
acetone	-5.32	+2.75

Table 4.8 Average solvent induced gap closure ($\Delta\Delta E_{int}$, kcal·mol^{-1}) between (root 1-root 2) and (root 2-root3) respectively in the 81° twisted ethylene.

The decrease in the energy gap is more pronounced in polar solvents. This is a direct consequence of the charge separation in the excited state which leads to enhanced electrostatic interactions between solvent and solute in this state. The energy gap between the two excited (nearly degenerate) states is not influenced by apolar solvents. In polar solvents however, the charge separation that occurs causes a distinct energy splitting between these two states. This is of course mainly caused by the electrostatic interactions between the polarized ethylene and the solvent. This interaction is attractive for the lower state while it is repulsive for the second excited state.

4.4 Summary and Conclusion

All valence CISD calculations at the 81˚ twist angle of ethylene using the Dunning-Huzinaga DZV basis were performed, embedding the quantum system in a discrete classical surrounding using the Direct Reaction Field Model. The classical surrounding consisted of 50 discretely described solvent molecules, each fitted with a molecular polarizability. 20 different solvent configurations were selected from a fully classical Monte Carlo simulation. This procedure was performed using ethane, tetrachloromethane, carbon dioxide, chloroform and acetone as solvents.

The 81˚ twist angle was chosen from a finite field study using the same wave function in vacuo. At this angle the excited state polarizability of the twisted ethylene proved to be the largest in this basis set, making this geometry the most likely candidate to be used for solvent induced sudden polarization studies.

The DRF studies revealed that the expectation value of the ethylenic excited state dipole moments remain small in the investigated non-polar solvents, ~±0.1 D in ethane and ~ ±0.7 D in tetra. Furthermore, the degeneracy of the two excited states was not lifted in these solvents which indicates that these solvents are not capable of breaking the symmetry of the excited state wave functions to a large extent. It can therefore be concluded that nonpolar solvents are unlikely to induce the sudden polarization in the twisted excited states of ethylene and that some sort of intramolecular symmetry breaking is required to generate the zwitterionic states.

The solvent-induced stabilization of the degenerate excited states with respect to the biradicaloid ground state is solely governed by the enhanced dispersion interaction with the solvent for these states. Even though this has to be treated with some caution, due to the approximate way this interaction is calculated, it is in agreement with intuitive concepts based on the assumed larger polarizabilities of excited states in general in comparison to their electronic ground state configuration.

A marked difference with the behavior mentioned above was observed in the more polar solvents chloroform, carbon dioxide and acetone. In these solvents, significant dipole moments (> 2 D) were generated in the ethylenic excited states. For the weakly polar chloroform there were still significant fluctuations between the values in various solvent configurations.

The more polar carbon dioxide and acetone showed a more pronounced polarization of the ethylene excited states, in (nearly) all investigated solvent configurations. In addition, a significant lift of the degeneracy of the two excited states was observed in these solvents (Table 4.8). This splitting between the two excited states is

most pronounced in acetone (~2 kcal·mol^{-1}). Analysis of the various contributions to the interaction energy show that the difference in electrostatic interaction with the solvent is mainly responsible for this splitting. Interestingly, the induction interaction had no significant influence on this process, suggesting that the polarity rather than the polarizability of the solvent is responsible for the symmetry breaking.

It can therefore be concluded that polar solvents are capable of breaking the symmetry of the ethylene excited states even when the alkene exhibits a symmetrical (i.e. unpyramidalized) nuclear configuration. It is emphasized that in all cases the surrounding solvent shells were in equilibrium with an unpolarized charge distribution. The inclusion of solvent relaxation will lead to more pronounced differences in excited state energies in cases where large dipoles are being generated and stabilized. Although beyond the scope of this work, this is an interesting topic to address in the future since the solvent-dependent narrowing of the gap between ground and excited state has been used as an explanation for the shortened lifetimes of the excited states in for instance tetraphenylethylene (TPE) as a function of increasing solvent polarity.

In experimental studies performed on the excited state behavior of TPE and other symmetrical olefins, it is usually assumed that the electronic structure of the twisted excited states of these alkenes was zwitterionic of nature due to an intramolecular symmetry breaking. The results of this work show that the solvent plays a very important role in the symmetry breaking. This is especially relevant for substituted symmetrical ethylenes since in these cases the steric repulsion between the substituents will make intramolecular symmetry breaking by pyramidalization rather unlikely, as has been reported in chapter 2.

4.5 Appendix

Atomic polarizabilities (A.U.) and VanderWaals Radii (Bohr)

C	8.6959	3.4015
H	2.7927	1.5118
O	5.7494	3.0236
Cl	16.1979	4.3240

CHELPG Derived Partial Charges (A.U.)

Acetone

C	-0.3276	-0.3289	0.7153
H	0.0828	0.0831	0.0928
O	-0.5751		

Chloroform

C	-0.1250
H	0.2300
Cl	-0.0350

Tetrachloromethane

C	-0.2440
Cl	0.0610

Carbondioxide

C	0.9092
O	-0.4546

Ethane

C	0.0150
H	-0.0050

Ethene (used in Monte Carlo solvent configuration generation)

C	-0.0962
H	0.0481

4.6 References

1. R.S. Mulliken, Phys. Rev., **41**, 751-758 (1932).
2. G. Wald, Science, **162**, 230-239 (1968).
3. Q. Wang, R.W. Schoenlein, L.A. Peteanu, R.A. Mathies and C.V. Shank, Science, **266**, 422-424 (1994).
4. C.E. Wulfman and S. Kumei, Science, **172**, 1061 (1971).
5. V. Bonacic-Koutecky, P. Bruckmann, P. Hiberty, J. Koutecky, C. Leforestier and L. Salem, Angew. Chem., Int. Ed. Engl., **14**, 575-576 (1975).
6. L. Salem and W-D. Stohrer, J. Chem. Soc. Chem. Commun., 140-143 (1975).
7. L. Salem and P. Bruckmann, Nature, **258**, 526-528 (1975).
8. L. Salem, Acc. of Chem. Res., **12**, 87-92 (1979).
9. R.J. Buenker and S.D. Peyerimhoff, Chem. Phys., **9**, 75-89 (1976).
10. R.J. Buenker, V. Bonacic-Koutecky and L. Pogliani, J. Chem. Phys., **73**, 1836-1849 (1980).
11. P. Bruckmann and L. Salem, J. Am. Chem. Soc., **98**, 5037-5038 (1976).
12. V. Bonacic-Koutecky, J. Am. Chem. Soc., **100**, 396-404 (1978).
13. B.R. Brooks and H.F Schaefer III, J. Am. Chem. Soc., **101**, 307-311 (1979).
14. G. Orlandi, P. Palmieri and G. Poggi, J. Am. Chem. Soc., **101**, 3492-3497 (1979).
15. M. Persico, J. Am. Chem. Soc., **102**, 7839-7845 (1980).
16. R.P. Johnson and M.W. Schmidt, J. Am. Chem. Soc., **103**, 3244-3249 (1981).
17. I. Nebot-Gil and J-P. Malrieu, Chem. Phys. Lett., **84**, 571-574 (1981).
18. I. Nebot-Gil and J-P. Malrieu, J. Am. Chem. Soc., **104**, 3320-3325 (1982).
19. V. Bonacic-Koutecky, M. Persico, D. Döhnert and A. Sevin, J. Am. Chem. Soc., **104**, 6900-6907 (1982).
20. I.D. Petsalakis, G. Theodorakopoulos and C.A. Nicolaidis, J. Chem. Phys., **81**, 5952-5956 (1984).
21. I.D. Petsalakis, G. Theodorakopoulos, C.A. Nicolaidis, R.J. Buenker and S.D. Peyerimhoff, J. Chem. Phys., **81**, 3161-3167 (1984).
22. I.D.L. Albert and S. Ramasesha, J. Phys. Chem., **94**, 6540-6543 (1990).
23. P. Piotrowiak, Chem. Phys. Lett., **241**, 387-392 (1995).
24. R.W.J. Zijlstra, A.H. de Vries and P.Th. van Duijnen, Chem. Phys., **204**, 439-446 (1996).
25. M. Merchán and R. González-Luque, J. Chem. Phys., **106**, 1112-1122 (1997).
26. V. Molina, M. Merchán and B.O. Roos, J. Phys. Chem. A, **101**, 3478-3487 (1997).
27. J.A. Marshall, Science, **170**, 137-141 (1970).
28. B.I. Greene, Chem. Phys. Lett., **79**, 51-53 (1981).
29. P.F. Barbara, S.D. Rand and P.M. Rentzepis, J. Am. Chem. Soc., **103**, 2156-2162 (1981).
30. B.H. Baretz, A.K. Singh and R.S.H. Liu, Nouv. J. Chim., **5**, 297-303 (1981).
31. F.E. Doany, E.J. Heilweil, R. Moore and R.M. Hochstrasser, J. Chem. Phys., **80**, 201-206 (1984).
32. A.G. Doukas, M.R. Junnarkar, R.R. Alfano, R.H. Callender, T. Kakitani and B. Honig, Proc. Natl. Acad. Sci. USA, **81**, 4790-4794 (1984).
33. W. Rettig, Angew. Chem., Int. Ed. Engl., **25**, 971-988 (1986).

34. E. Gilabert, R. Lapouyade and C. Rullière, Chem. Phys. Lett., **145**, 262-268 (1988).
35. C.L. Schilling and E.F. Hilinski, J. Am. Chem. Soc., **110**, 2296-2298 (1988).
36. H. Ephardt and P. Fromherz, J. Phys. Chem., **93**, 7717-7725 (1989).
37. C.T. Lin, H.W. Guan, R.K. McCoy and C.W. Spangler, J. Phys. Chem., **93**, 39-43 (1989).
38. D.B. Toublanc, R.W. Fessenden and A. Hitachi, J. Phys. Chem., **93**, 2893-2896 (1989).
39. J. Morais, J. Ma and M.B. Zimmt, J. Phys. Chem., **95**, 3885-3889 (1991).
40. D.H. Waldeck, Chem. Rev., **91**, 415-436 (1991).
41. R. Lapouyade, K. Cheschka, W. Majenz, W. Rettig, E. Gilabert and C. Rullière, J. Phys. Chem., **96**, 9643-9650 (1992).
42. S. Marguet, J.C. Mialocq and P. Millie, Chem. Phys., **160**, 265-279 (1992).
43. J. Ma and M.B. Zimmt, J. Am. Chem. Soc., **114**, 9723-9724 (1992).
44. W. Schuddeboom, S.A. Jonker, J.M. Warman, M.P. de Haas, M.J.W. Vermeulen, W.F. Jager, B. de Lange, B.L. Feringa and R.W. Fessenden, J. Am. Chem. Soc., **115**, 3286-3290 (1993).
45. L. Sun and H. Görner, Chem. Phys. Lett., **208**, 43-47 (1993).
46. J-M. Rodier and A.B. Myers, J. Am. Chem. Soc., **115**, 10791-10795 (1993).
47. J. Ma, G. Bhaskar Dutt, D.H. Waldeck and M.B. Zimmt, J. Am. Chem. Soc, **116**, 10619-10629 (1994).
48. J. Saltiel, D-H. Ko and S.A. Fleming, J. Am. Chem. Soc., **116**, 4099-4100 (1994).
49. K. Sandros and M. Sundahl, J. Phys. Chem., **98**, 5705-5708 (1994).
50. Y-P. Sun and C.E. Bunker, J. Am. Chem. Soc., **116**, 2430-2433 (1994).
51. T. Tahara and H. Hamaguchi, Chem. Phys. Lett., **217**, 369-374 (1994).
52. J-M. Viallet, F. Dupuy, R. Lapouyade and C. Rullière, Chem. Phys. Lett., **222**, 571-578 (1994).
53. E. Lenderink, K. Duppen and D.A. Wiersma, J. Phys. Chem., **99**, 8972-8977 (1995).
54. P. Piotrowiak, G. Strati, J. Warman and W. Schuddeboom, J. Am. Chem. Soc., **118**, 8981-8982 (1996).
55. J. Saltiel, Y. Zhang and D.F. Sears Jr., J. Am. Chem. Soc., **119**, 11202-11210 (1997).
56. R.W.J. Zijlstra, P. Th. van Duijnen, B.L. Feringa, T. Steffen, K. Duppen and D.A. Wiersma, J. Phys. Chem. A, **101**, 9828-9836 (1997).
57. L. Salem, Science, **191**, 822-830 (1976).
58. V. Bonacic-Koutecky, J. Cizek, D. Döhnert and J. Koutecky, J. Chem. Phys., **69**, 1169-1176 (1978).
59. V. Bonacic-Koutecky, R.J. Buenker and S.D. Peyerimhoff, J. Am. Chem. Soc., **101**, 5917-5922 (1979).
60. C.E. Wulfman and G.C. Hyatt, Proc. Indian Acad. Sci. (Chem. Sci.), **107**, 813-823 (1985).
61. M.L. Connolly, Science, **221**, 709-713 (1983).
62. B.T. Thole and P. Th. van Duijnen, Theor. Chim. Acta, **55**, 307-318 (1980).
63. P. Th. van Duijnen, A.H. Juffer and H.P. Dijkman, J. Mol. Struct. (THEOCHEM), **260**, 195-205 (1992).

64. A.H. de Vries, P.Th. van Duijnen, J.A.C. Ruhlmann, J.P. Dijkman, H. Merenga and B.T. Thole, J. Comp. Chem., **16**, 37-55 (1995).
65. P. Th. van Duijnen and A.H. de Vries, Int. J. Quant. Chem., **60**, 1111-1132 (1996).
66. A.H. de Vries and P. Th. van Duijnen, Int. J. Quant. Chem., **57**, 1067-1076 (1996).
67. T.H. DunningJr. and P.J. Hay, *Gaussian basis sets*, in: Methods of Electronic Structure Theory, Ed: H. F. Schaeffer. III, 1977.
68. P. Th. van Duijnen and M. Swart, J. Phys. Chem. A, **102**, 2399-2407 (1998).
69. B.T. Thole and P. Th. van Duijnen, Theor. Chim. Acta, **63**, 209-221 (1983).
70. M.P. Allen and D.J. Tildesley, *Computer Simulation of Liquids*, Clarendon Press, Oxford, 1987.
71. R.C. Weast, M.J. Astle and W.H. Beyer, *Handbook of Chemistry and Physics*, CRC Press Inc., Boca Raton, Fl., USA, 1985-1986.
72. H.D. Cohen and C.C.J. Roothaan, J. Chem. Phys., **43**, S34-S39 (1965).
73. H.A. Kurtz, J.J.P. Stewart and K.M. Dieter, J. Comp. Chem., **11**, 82-87 (1990).
74. M. Dupuis, A. Farazdel, S.P. Karma and S.A. Maluendes, *HONDO: A General Atomic and Molecular Electronic Structure System*, in: MOTECC, Ed: E. Clementi, ESCOM, Leiden, The Netherlands, 1990.